Electronic Appendix 2

Table A1.1: FTIR absorbance measurements, sample thicknesses, and glass densities of experimental glasses.

Sample[1]	A_{1430}	A_{1525}	A_{4500}	A_{5200}	A_{1640}	A_{3500}	A_{2345}	d (μm)	ρ (g/L)
AW-82038 Phonotephrite Experiments									
AW-06-a	0.190	0.191			0.137	0.815		66	2538.93
AW-06-b	0.142	0.181			0.103	0.861		65	2538.93
AW-10-a					0.449	1.292		27.5*	2348.18
AW-10-b					0.520	1.446		31.6*	2348.18
AW-13-a					0.205	0.765		20.5*	2443.39
AW-13-b	0.041	0.048			0.176	0.654		17.5*	2443.39
AW-13-c					0.202	0.594		17.2*	2443.39
AW-13-d	0.029	0.030			0.250	0.953		24.7*	2443.39
AW-14-a	0.192	0.207	0.019		0.776	2.131	0.049	124	2605.45
AW-14-b			0.020					124	2605.45
AW-17-a	0.049	0.060	0.011	0.008	0.372	1.785		63	2502.23
AW-17-b	0.052	0.061	0.011	0.008	0.358	1.739		61	2502.23
AW-17-c	0.049	0.071	0.012	0.008	0.395	1.739		65	2502.23
AW-19B-a						0.291		68	2438.59
AW-20B-a	0.036	0.043			0.105	0.353	0.028	23	2411.85
AW-21-a			0.006	0.005	0.177	0.505		17.1*	2666.52
AW-21-b					0.175	0.587		20.2*	2667.09
AW-21-c					0.147	0.651		19.7*	2662.15
AW-21-d	0.025	0.033						15.9*	2662.15
AW-22-a	0.053	0.042				1.002		27.3*	2693.37
AW-22-b				0.014	0.285	0.948		23.1*	2687.8
AW-22-c					0.315	1.002		27.7*	2694.15
AW-23-a					0.488	1.248		27.4*	2270.11
AW-23-b					0.465	1.218		27.7*	2270.11
AW-23-c					0.426	1.119		25.0*	2270.11
AW-24-a	0.618	0.602			0.287	1.850		174	2613.8
AW-24-b	0.611	0.602			0.316	1.805		174	2613.8
AW-24-c	0.653	0.657			0.349	1.839		174	2613.8
AW-25-a	0.247	0.273	0.014	0.008	0.351	1.948		92	2588.6
AW-25-b	0.266	0.295	0.015	0.010	0.385	2.103		96	2588.6
AW-25-c	0.194	0.205	0.010	0.007	0.272	1.623		82	2588.6
AW-25-d	0.182	0.191	0.010	0.006	0.256	1.512		76	2588.6
AW-25-e	0.191	0.200	0.012	0.008	0.275	1.646		80	2588.6
AW-25-f	0.216	0.239	0.011	0.007	0.317	1.785		86	2588.6
AW-26-a	0.103	0.111	0.009	0.010	0.505	1.809		57	2498.74
AW-26-b	0.116	0.116	0.009	0.010	0.520	1.832		57	2498.74
AW-26-c	0.125		0.01	0.009	0.52	1.855		59	2498.74
AW-26-d	0.116	0.129	0.01	0.01	0.52	1.855		58	2498.74

Table A1.1 Continued

AW-27-a	0.207	0.224			1.395		89	2543.54
AW-27-b	0.263	0.267	0.009	0.016	1.412		93	2543.54
AW-27-c	0.321	0.344	0.016	0.027	1.576		94	2543.54
AW-28-a			0.005	0.015	0.592	1.278	23.7*	2328.66
AW-28-b					0.494	1.173	24.9*	2328.66
AW-28-c					0.533	1.248	22.9*	2328.66
AW-28-d					0.476	1.145	17.9*	2328.66
AW-29-a	0.178	0.161				0.415	45	2657.97
AW-29-b						0.432	45	2657.97
AW-29-c	0.145	0.153				0.437	45	2657.97
AW-33-a	0.111	0.122			0.148	0.805	30	2520.2
AW-33-b	0.117	0.135			0.163	0.842	32	2520.2
AW-33-c	0.078	0.091			0.123	0.823	32	2520.2
AW-34-a			0.035	0.018	1.260		95	2414.79
AW-34-b			0.033	0.016	1.218		91.3*	2414.79
AW-34-c			0.036	0.015	1.333		91*	2414.79
AW-34-d			0.082	0.045			178	2414.79
AW-38-a					0.169	0.361	6.1*	2224.75
AW-38-b					0.205	0.495	8.1*	2224.75
AW-38-c					0.151	0.433	7.4*	2224.75
AW-39-a	0.312	0.336	0.019	0.035	1.341		110	2409.74
AW-39-b	0.211		0.016	0.037	1.297		110	2409.74
AW-39-c			0.020	0.033	1.218		110	2409.74
AW-39-d			0.023	0.032	1.484		110	2409.74
AW-40-a	0.268	0.268	0.013	0.010			89	2532.21
AW-40-b	0.341	0.345	0.014	0.011	0.545		89	2532.21
AW-40-c	0.390	0.405	0.017	0.014	0.630		89	2532.21
AW-40-d	0.380	0.386	0.015	0.013			89	2532.21
AW-41-a	0.388	0.382	0.020	0.014	0.504		176	2537.76
AW-42-a	0.219	0.190			0.126	0.675	97	2550.42
AW-42-b	0.127	0.124			0.078	0.437	68	2550.42
AW-42-c						0.463	71.4*	2550.42
AW-44-a						1.373	75	2330.42
AW-45-a	0.677	0.664	0.020	0.026	1.123		110	2332.19
AW-45-b	0.904	0.860	0.023	0.025	1.224		110	2332.19
AW-45-c	0.568	0.568	0.021	0.027	1.072		110	2332.19
AW-45-d	0.540	0.497			0.868		110	2332.19
AW-45-e			0.020	0.026			110	2332.19
AW-46-a	0.348		0.012	0.024	0.879	2.050	58	2093.46
AW-46-b	0.348		0.014	0.030	1.148		58	2093.46
AW-46-c	0.373		0.014	0.030	1.059		58	2093.46
AW-47-a						1.139	18.4*	2688.56

Table A1.1 Continued

AW-47-b						1.139	16.7*	2680.29
KI-04 Basanite Experiments								
KI-07-a	0.130	0.166			0.257	1.563	52	2820.18
KI-07-b	0.117	0.143	0.008	0.006	0.227	1.496	52	2820.18
KI-07-c	0.126	0.154	0.009	0.006	0.247	1.546	55	2820.18
KI-07-d	0.149	0.175	0.008	0.006	0.267	1.576	54	2820.18
KI-09-a	0.091	0.094			0.041	0.239	44	2629.61
KI-09-b	0.089	0.079				0.289	44	2629.61
KI-09-c					0.056	0.250	41	2629.61
KI-09-d	0.123	0.141			0.029	0.404	45	2629.61
KI-10-a	0.101	0.098			0.212	0.533	37	2672.91
KI-10-b	0.087	0.104			0.174	0.571	37	2672.91
KI-10-c	0.104	0.130			0.197	0.491	37	2672.91
KI-15-a	0.631	0.631			0.230	1.412	75.6*	2778.91
KI-15-b	0.403	0.429			0.169	1.263	66.7*	2778.91
KI-16-a	0.513	0.480			0.491	1.582	50	2682.22
KI-20-a	0.096	0.099			0.265	0.737	29	2798.31
KI-20-b	0.132				0.194	0.580	29	2798.31
KI-20-c	0.111	0.117			0.260	0.590	29	2798.31
KI-21-a	0.325	0.314			0.202	0.906	40	2731.74
KI-21-b	0.186	0.188			0.134	0.779	40	2731.74
KI-21-c	0.113	0.117			0.129	0.601	20.3*	2731.74
KI-21-d	0.140	0.148			0.126	0.659	20.8*	2731.74
KI-21-e	0.145	0.170			0.174	0.678	21.4*	2731.74
KI-23-a	0.553	0.559	0.017		0.032	0.908	78	2831.76
KI-23-b	0.494	0.501			0.013	0.886	78	2831.76
KI-23-c	0.432	0.443	0.009	0.007	0.032	0.851	78	2831.76
KI-23-d	0.481	0.501	0.012	0.006	0.078	0.833	78	2831.76
KI-32-a	0.119				0.399	0.944	34	2556.2
KI-32-b	0.117				0.398	0.950	34	2556.2
KI-32-c	0.132				0.397	0.950	34	2556.2
KI-32-d	0.107				0.357	0.917	34	2556.2
KI-07-a	0.130	0.166			0.257	1.563	52	2820.18
KI-07-b	0.117	0.143	0.008	0.006	0.227	1.496	52	2820.18

[1]Capital letters and numbers refer to experiment type and number. Lowercase letter refers to individual FTIR measurement. *Refers to sample thicknesses measured by interference fringes (see text). d = sample thickness; ρ = glass density.

Details of FTIR spectral background fitting

Spectral backgrounds were determined by fitting computer-generated polynomial curves to selected sections of the FTIR spectra. Typically, 5200 and 4500 cm^{-1} OH peaks were measured relative to a second order polynomial background, the 3500 cm^{-1} total water peak was assumed to have a straight-line background, and the 1640 water peak and the 1525 and 1430 cm^{-1} carbonate doublet were measured relative to a 4^{th} or 5^{th} order polynomial background (see example spectra in Figure A1.1). A background curve fit for the molecular water and carbonate peaks was deemed best when the heights of the 1525 and 1430 cm^{-1} peaks were closest in value, as these two peaks form the carbonate doublet and should be roughly equivalent. Some backgrounds were additionally hand drawn using a French curve, which gave similar results to the computer-generated background fits. The code used to generate curve fits (Iacovino, 2014) was an early version of an FTIR retrieval program (Iacovino & Peters, in preparation; Iacovino et al., 2013b) written as a plug-in to the extensible plotting tool AvoPlot (Peters, 2014) and can be downloaded at http://dx.doi.org/10.6084/m9.figshare.928142.

Sample thickness measurement via interference fringes

Sample thickness was typically measured using a tabletop micrometer (see main text). Several spots on the sample surface were measured with the aim of producing a representative thickness, but the transfer of sample from spectrometer to gauge always creates some uncertainty as to whether the thickness measurement corresponds to the actual sample area analyzed. For thin samples in particular, there is the added risk of crushing the sample during thickness measurement. In our thinnest samples, the presence

of interference fringes in reflection IR spectra allowed for the measurement of sample thickness following the method in Nichols and Wysoczanski (2007; and references therein). Because the spectrometer can be switched from transmission to reflection mode without movement of the sample, thickness can be measured in the exact spot measured for the retrieval of volatile concentrations. Typical transmission and reflection spectra for thin samples are shown in Figure A1.2. For these calculations, we assume a refractive index of 1.51 for phonotephrite experiments (Church and Johnson 1980) and 1.569 for basanite experiments (value for tholeiite glass at low P; Kuryaeva and Kirkinskii 1997). Only these two values were used, as the refractive index is not expected to change much as melt composition evolves.

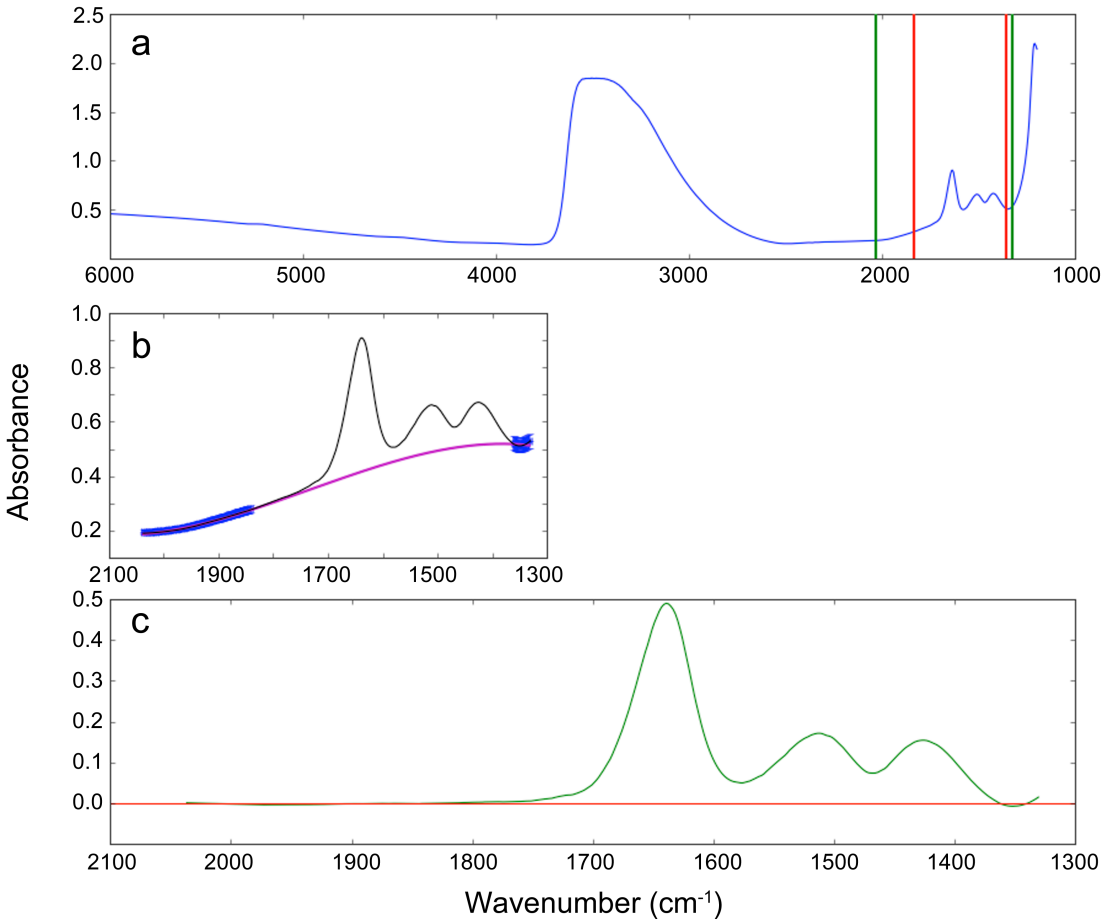

Figure A1.1 Example showing how the computer program was used to determine background fits (shown: sample AW-40). (a) A user-defined region of the spectrum over which to fit a background is defined by the green and red bars where the program will fit a polynomial to any points within the green bars but excluding the points within the red bars. (b) A window is displayed showing the background fit (purple) with no correction applied to the original spectrum (black). Blue points are those chosen in (a) plus error bars within which the curve fit is deemed acceptable. (c) A third window shows the background-corrected spectrum (green) and the background fit (red), which is set equal to zero. Numbers on the y-axis in (c) indicate background-corrected values.

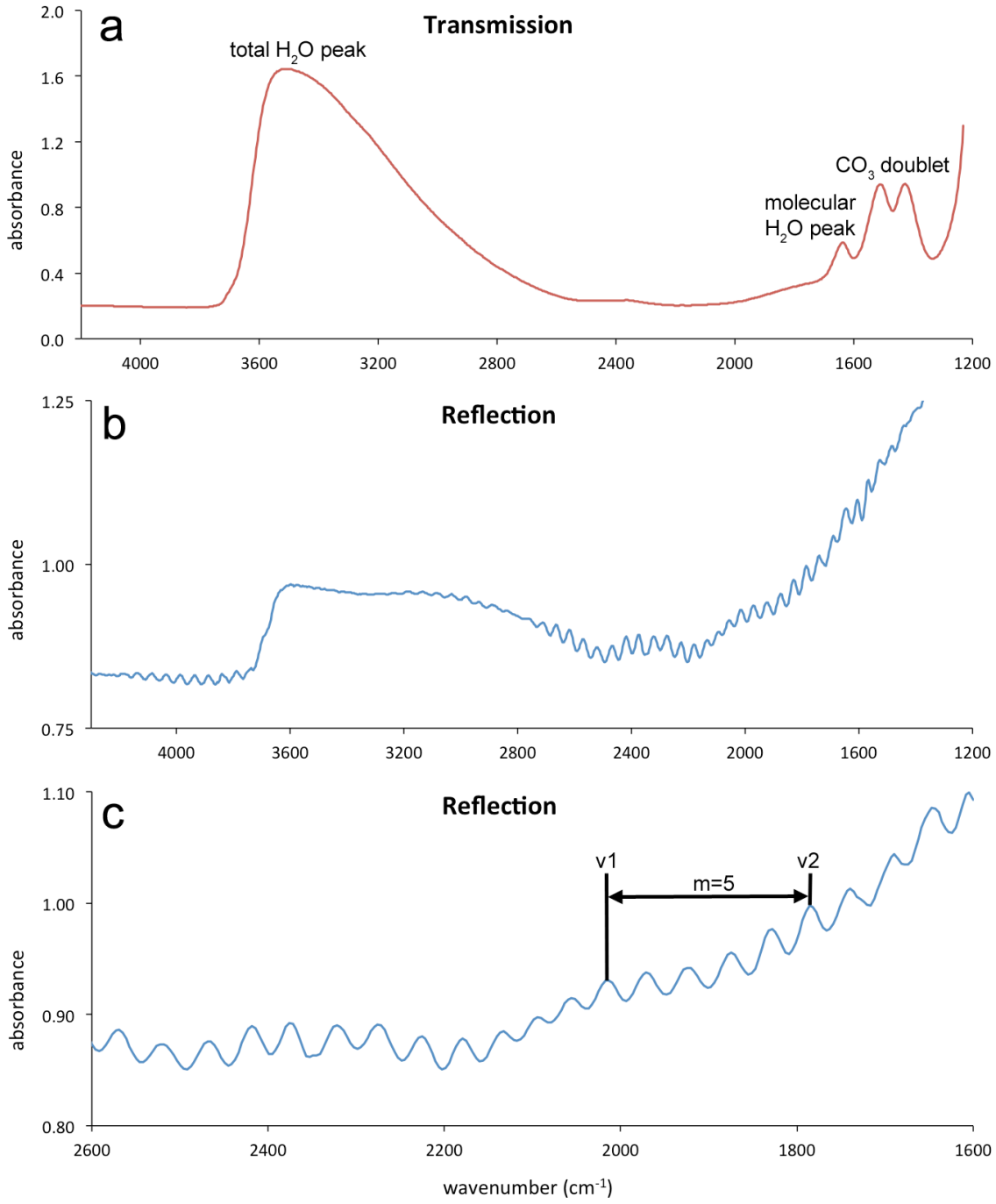

Figure A1.2 Representative spectra of transmission (a) and reflection (b and c) FTIR measurements in thin samples (shown: sample KI-15). (a) H_2O and CO_2 were measured using the bands at 3500 cm^{-1} (total H_2O), 1640 cm^{-1} (molecular H_2O), 1430 and 1525 cm^{-1} (CO_3), 2345 cm^{-1} (CO_2, when present), and near IR (not shown). (b) Reflection spectrum taken at the same spot as (a) showing interference fringes. (c) Following the method described in Nichols and Wysoczanski (2007), the number of interference fringes, *m*, over a given wavenumber range from *v1* to *v2* were used to determine sample thickness.